Supporting Information

Kucyi et al. 10.1073/pnas.1312902110

SI Methods

Exclusion Criteria and Informed Consent. Exclusion criteria included history of neurological/psychiatric/chronic illness, regular pain in the last 6 mo, and medication use (besides birth control). Informed written consent was obtained for procedures approved by the University Health Network Research Ethics Board.

Session 1 (Psychophysics) Procedures. Electrodes connected to a 300-PV (Empi Inc.) transcutaneous electrical nerve stimulation (TENS) device were placed over the median nerve of the participant's left forearm with saline paste to improve conduction. Current was delivered using a symmetric waveform at 50 Hz (pulse width of 250 μs). Current level was gradually increased while the participant verbally rated pain intensity on a scale from 0 (no pain) to 10 (most intense pain imaginable). The level evoking a rating of 4–5 was used in subsequent procedures.

The participant next completed a series of tasks displayed on a computer with EPrime v1.1 (Psychology Software Tools). Painful stimuli were delivered at predetermined intervals with an Arduino microcontroller (Smart Projects) that connected the TENS device with the computer. The participant first continuously rated pain intensity during a 20-s stimulus, repeated twice. Ratings were performed with a trackball while the participant viewed a visual analog scale anchored from 0 (no pain) to 10 (most intense pain imaginable). The experimenter monitored these continuous ratings to ensure that stimuli consistently evoked ratings of 4–5 out of 10. Current level was readjusted if there were deviations. Next, the participant completed the experience sampling and cognitive interference tasks (described below). The order of these two tasks was counterbalanced across participants. All 51 participants completed experience sampling in the psychophysics session (20 trials each, except one participant who completed 19 trials due to acquisition error). After performance of the two tasks, the participant completed questionnaires: (*i*) pain catastrophizing scale (1) and (*ii*) daydreaming frequency scale of the Imaginal Process Inventory (2).

Session 2 (Neuroimaging) Procedures. Participants returned on day 2 for neuroimaging (mean number of days between sessions ± SD = 4.8 ± 3.4) with a 3T GE MRI system including an eight-channel phased array head coil. Before scanning, TENS electrodes were set up as in session 1, and current level was set to evoke a pain intensity rating of 4–5. Scans included one run of resting state functional magnetic resonance imaging (fMRI) followed by four runs of fMRI with the experience sampling task and diffusion-weighted MRI (DWI). Two T_1-weighted anatomical scans were collected, one before fMRI and one before DWI. During the first T_1-weighted and fMRI scans, the participant wore goggles to view EPrime displays, and a four-button Fiber Optic Response Pad (Current Designs) was placed in the right hand. Earplugs were worn during all scans. Fifty participants completed experience sampling during the fMRI session (47 participants completed 40 trials; due to acquisition errors, two participants completed 30 trials, one completed 39 trials, and one did not participate).

The imaging acquisition parameters were as follows: first T_1-weighted scan (matrix = 256 × 256; 104 axial slices; 0.78 × 0.78 × 1.5 mm^3 voxels; flip angle = 20°; echo time (TE) = 3 ms; repetition time (TR) = 7,800 ms; inversion time (TI) = 300 ms), T_2*-weighted echo-planar fMRI scans (matrix = 64 × 64; 36 axial slices per volume; 3.125 × 3.125 × 4 mm^3 voxels; interleaved slice acquisition; no gap; flip angle = 90°; TE = 30 ms; TR = 2,000 ms; number of volumes = 266), second T_1-weighted scan (matrix = 256 × 256, 176 axial slices; 1 × 1 × 1 mm^3 voxels; flip angle = 15°; TE = 3 ms; TR = 7,800 ms; TI = 450 ms) and DWI (matrix = 96 × 96; 64 axial slices per volume; 2.4 × 2.4 × 2.4 mm^3 voxels; b = 1,000 s/mm^2; 60 diffusion-encoding directions; 10 non–diffusion-weighted B0 images; TE = min; TR = 17,000 ms). For the resting state fMRI scan, 277 volumes were collected (9 min 14 s) and the subject was instructed "close your eyes; do not try to think about anything in particular; do not fall asleep." For each task fMRI scan, 266 volumes were collected (8 min 52 s).

Experience Sampling Task Instructions and Details. Both during psychophysics and imaging (fMRI) sessions, an experience sampling task was performed. The participant received the following instructions to minimize active efforts to attend toward or away from pain:

> Now we will again deliver electrical stimuli to your nerve to induce pain, and we are testing how your mind may wander toward and away from pain. During the upcoming painful stimulation, please keep focused on the cross in the center of the screen and do not try to think about anything in particular. Avoid structured thinking such as counting or singing. As soon as stimulation stops, a question will appear on the screen asking you what you were just feeling and thinking of immediately prior to the end of stimulation. For example, you might have just been noticing, experiencing and feeling pain, but you might have been thinking of something completely unrelated to pain and perhaps then did not notice or fully feel the pain.

Between runs (10 trials each), the participant reported whether the pain intensity evoked by TENS was still 4–5. Readjustments in electrical current were made if necessary.

Cognitive Interference Task: Procedures and Analysis. We used a cognitive interference task previously shown in our laboratory to identify behavioral phenotypes that distinguish individuals who prioritize attention over pain (A type) from individuals in whom pain dominates during task performance (P type) (3). On each trial, three adjacent boxes were displayed, each containing varying numbers of digits that ranged in value between 1 and 9. Participants were instructed to find the box containing the greatest number of digits (i.e., highest count) and report that number on a numeric keypad with their right hand. Participants were told to respond as quickly as possible while also maintaining accuracy and were told to neither attend to nor ignore painful stimulation. Each trial lasted 2.5 s, with no intertrial interval. Four blocks of practice trials were run, followed by the test blocks. Each block contained 24 trials, and blocks were presented with 60-s interblock intervals. Concurrent TENS was delivered during every second block. Four different versions of the task with randomized trial orders were used, with versions counterbalanced across participants.

We calculated the difference between mean reaction time (RT) across pain versus no-pain trials (ΔRT [P − NP]) to quantify interference of pain with performance (3, 4). Error trials and outlier trials (defined as within-block z score >2 or <−2) were excluded. Three participants were excluded from analyses of this task [one who performed all trials incorrectly, one who performed poorly and had an insufficient number of correct trials to be analyzed (i.e., overall error rate > 40%), and one extreme outlier with a ΔRT [P − NP] of 448.9 ms (5.3 SDs from the group mean)].

Task fMRI: Analysis Inclusion Criteria, Preprocessing, and Analysis. For contrasts of intraindividual fMRI activity during "pain" and "else" reports, only participants with sufficient frequencies of the two responses (with "only" and "mostly" responses binned

together) were included. Participants who reported at least two trials of a given category within at least three of the four runs were included. Three and four runs were used for 10 and 22 participants, respectively, resulting in 572 pain and 608 else total trials across 32 participants. For all included fMRI runs, preprocessing included deletion of the first five volumes, motion correction with FMRIB's linear registration tool (FLIRT), brain extraction, spatial smoothing (6-mm FWHM), and high-pass temporal filtering (0.01-Hz cutoff). Linear registration [FLIRT, six degrees of freedom (DOF)] to T_1-weighted image and Montreal Neurological Institute standard space was performed.

For each run, a first-level general linear model (GLM) with FMRIB's improved linear model prewhitening included three regressors convolved with a gamma hemodynamic response function (gHRF): 20-s pain stimulation periods before pain reports, 20-s pain stimulation periods before else reports, and 8-s rating periods. Contrasts were performed to identify activation/deactivation during stimulation before pain and else reports as well as pain > else and else > pain differences. Across runs and for each contrast, second-level within-subject fixed effects analyses were performed. A third-level (group) analysis was performed with FMRIB's local analysis of mixed effects (FLAME) 1 + 2 (thresholding: whole-brain family-wise error (FWE)-corrected $Z > 2.3$; cluster $P < 0.05$). Average contrast of parameter estimate values were extracted from two 6-mm-radius spheres surrounding peak coordinates in the default network core (5) (posterior cingulate cortex and medial prefrontal cortex) identified from the else > pain contrast. Spearman's correlations were calculated between these values and individual differences in postscan ratings of the degree to which reports of "something else" were due to external sensory distractions (EDs), task-related interferences (TRIs), and mind wandering (MW).

The psychophysiological interaction (PPI) analysis (6) was performed with a seed region defined in the periaqueductal gray (PAG) (*xyz* MNI coordinates: 0, 32, 12; size: 6-mm-radius sphere) as was done previously (7). The seed was transformed to native space. The average time course across seed voxels was extracted from preprocessed images for each run. A first-level GLM with FILM prewhitening included the three gHRF-convolved regressors, as in the activation analysis, and three additional regressors: PAG time course, interaction between PAG time course and stimulation before pain reports, and interaction between PAG time course and stimulation before else reports. Contrasts were performed between two PAG interaction regressors (PAG time course × stimulation before pain reports and PAG time course × stimulation before else reports) to identify regions with pain > else and else > pain PAG functional connectivity. Second- and third-level analyses proceeded as in the activation analysis. To explore possible interactions of the default mode network, this PPI analysis was repeated with a seed region in the posterior cingulate cortex (PCC), defined as a 6-mm-radius sphere surrounding peak MNI coordinates (*xyz* = −8, −50, 28) obtained from the else > pain contrast from the activation analysis described above (Fig. S2).

Diffusion MRI Processing and Analysis. Preprocessing included motion correction, eddy current correction, and brain extraction. For probabilistic tractography, probability distributions were estimated at each voxel for two possible fiber orientations with Bayesian estimation of diffusion parameters obtained using sampling techniques (BEDPOSTX). Linear registration (FLIRT, six DOF) to T_1-weighted image and MNI standard space was performed. A seed was defined in the PAG (as in the PPI analysis), and a target was defined as a 6-mm-radius sphere surrounding peak coordinates in the medial prefrontal cortex (mPFC) derived from the contrast else > pain PAG functional connectivity in the PPI analysis. The pathway was restricted with use of the thalamic prefrontal radiation from the Oxford Thalamic Connectivity Probability Atlas as a waypoint (8) to optimize the specificity of the PAG–prefrontal pathway and remove spurious connections. Probabilistic tractography was performed with 5,000 streamline samples drawn on principal diffusion directions (curvature threshold = 0.2). A threshold was set to include only voxels with at least 500 samples passing through (8). Voxels were then binarized within individuals and summed across individuals. To remove voxels with low consistency across participants, this summed pathway was thresholded to include only voxels shared by at least five participants.

For tract-based spatial statistics, a diffusion tensor model was fitted at each voxel using a weighted least-squares approach to generate individual fractional anisotropy (FA) maps, which were transformed to the space of the FMRIB58_FA standard template via nonlinear registration and averaged across individuals. A thinned white matter "skeleton" representing the common center of tracts across individuals was created and thresholded at FA > 0.2. Each individual's peak FA value in tract voxels perpendicular to the skeleton was used for statistical analysis.

Resting State fMRI Preprocessing. The first four volumes of resting state fMRI were deleted, followed by motion correction (MCFLIRT) and linear registration (FLIRT, six DOF) to T_1-weighted image and MNI standard space. To remove physiological-/scanner-related noise, aCompCor procedures (9, 10) were performed. This included segmentation of the T_1-weighted image using FMRIB's automated segmentation tool v4.1 followed by registration of white matter (WM) and cerebrospinal fluid (CSF) partial volume maps to fMRI space. These maps were then eroded by thresholding to retain the top 198 cm^3 and top 20 cm^3 of voxels with highest probability of being WM and CSF, respectively (10). Voxels within the eroded WM and CSF volumes were then masked with the 4D fMRI data and submitted to principal components analysis. The top five WM components, top five CSF components, and six motion parameters obtained with MCFLIRT were regressed out of the motion-corrected fMRI data. Spatial smoothing (6-mm FWHM) and band-pass temporal filtering (0.01–0.1 Hz) were then performed. Regions of interest were defined in the PAG and mPFC in standard space as in the PPI and DWI analyses and were registered to fMRI space.

1. Sullivan MJ, Bishop SR, Pivik J (1995) The pain catastrophizing scale: Development and validation. *Psychol Assess* 7(4):524–532.
2. Singer JL, Antrobus JS, eds (1972) *The Function and Nature of Imagery* (Academic Press, New York), pp 175–202.
3. Erpelding N, Davis KD (2013) Neural underpinnings of behavioural strategies that prioritize either cognitive task performance or pain. *Pain* 154(10):2060–2071.
4. Seminowicz DA, Mikulis DJ, Davis KD (2004) Cognitive modulation of pain-related brain responses depends on behavioral strategy. *Pain* 112(1–2):48–58.
5. Andrews-Hanna JR, Reidler JS, Sepulcre J, Poulin R, Buckner RL (2010) Functional-anatomic fractionation of the brain's default network. *Neuron* 65(4):550–562.
6. Friston KJ, et al. (1997) Psychophysiological and modulatory interactions in neuroimaging. *Neuroimage* 6(3):218–229.
7. Eippert F, et al. (2009) Activation of the opioidergic descending pain control system underlies placebo analgesia. *Neuron* 63(4):533–543.
8. Stein N, Sprenger C, Scholz J, Wiech K, Bingel U (2012) White matter integrity of the descending pain modulatory system is associated with interindividual differences in placebo analgesia. *Pain* 153(11):2210–2217.
9. Behzadi Y, Restom K, Liau J, Liu TT (2007) A component based noise correction method (CompCor) for BOLD and perfusion based fMRI. *Neuroimage* 37(1):90–101.
10. Chai XJ, Castañón AN, Ongür D, Whitfield-Gabrieli S (2012) Anticorrelations in resting state networks without global signal regression. *Neuroimage* 59(2):1420–1428.

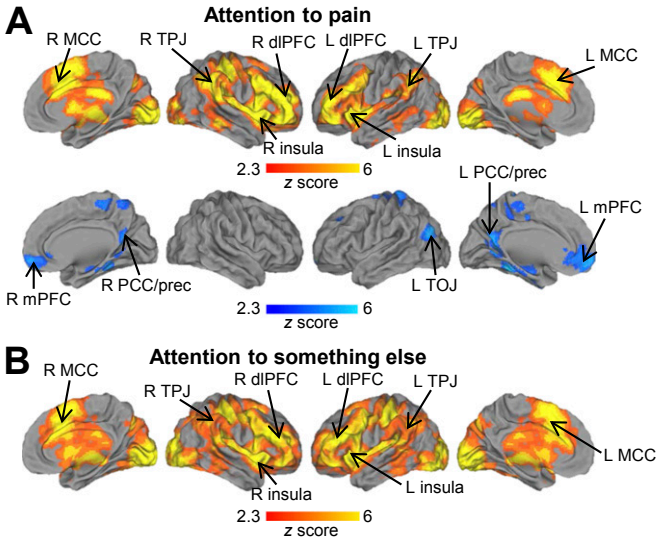

Fig. S1. Brain activations and deactivations (*A*) during painful stimulation preceding reports of attention to pain and (*B*) during painful stimulation preceding reports of attention to something other than pain. Regions exhibiting significant activation (red/yellow) and deactivation (blue) are thresholded at whole-brain FWE-corrected $Z > 2.3$ (cluster $P < 0.05$), projected onto the cortical surface with computerized anatomical reconstruction and editing toolkit (CARET). No significant deactivations were found during painful stimulation preceding reports of attention to something other than pain.

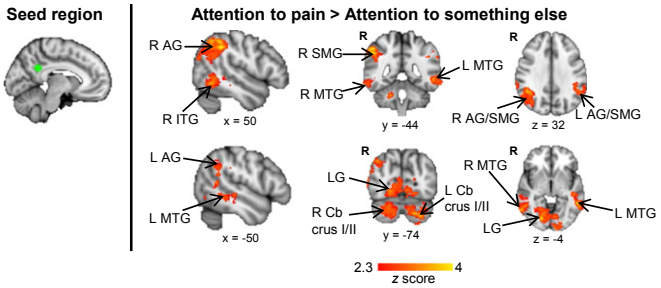

Fig. S2. Brain regions exhibiting significantly greater functional connectivity with the PCC (green) during attention to pain compared with attention to something else (red/yellow statistical image thresholded at whole-brain FWE-corrected $Z > 2.3$, cluster $P < 0.05$). No brain regions exhibited significantly greater functional connectivity with the PCC during attention to something else compared with attention to pain. AG, angular gyrus; Cb, cerebellum; ITG, inferior temporal gyrus; LG, lingual gyrus; MTG, middle temporal gyrus; SMG, supramarginal gyrus.

Table S1. Session 1 and 2 individual IAP scores and ratings for EDs, TRIs, and MW in 51 subjects

	IAP		EDs		TRIs		MW	
Subject	Session 1	Session 2	Session 1	Session 2	Session 1	Session 2	Session 1	Session 2
1	−1.05	−1.35	2	6	4	4	6	4
2	0.2	0.45	3	6	5	4	5	1
3	−0.9	−0.59	5	4	4	4	6	6
4	−0.16	0.025	5	6	5	2	4	2
5	0.7	1.125	5	6	4	4	2	5
6	1.25	1.025	4	3	4	3	2	2
7	0.3	−0.167	2	6	6	4	4	3
8	0.7	−0.1	2	2	2	1	6	5
9	0.1	−0.5	3	4	3	2	5	4
10	0.65	0.025	6	6	5	3	3	1
11	−0.75	−0.15	5	5	3	4	5	6
12	0.1	−0.33	1	2	5	3	4	6
13	−1.1	−0.7	1	3	5	4	4	4
14	0.1	0.15	1	3	4	5	4	5
15	0.75	0.5	1	4	2	2	6	3
16	1.8	1.575	1	4	5	5	1	2
17	0.95	−0.5	3	6	6	5	6	2
18	0.5	0.5	4	5	5	4	4	2
19	−0.3	0	1	3	1	3	6	6
20	1.15	1.275	5	4	4	4	3	2
21	−0.1	−0.275	2	2	3	3	6	6
22	−0.45	−1.225	2	3	5	3	5	4
23	0.2	−0.3	1	2	2	1	6	6
24	−0.3	0.2	1	2	1	3	7	4
25	0.15	0.1	6	6	5	5	3	2
26	1.6	0.725	3	3	5	5	3	3
27	0	−0.325	4	6	5	5	4	5
28	−0.15	−0.3	4	5	4	4	6	5
29	1.9	1.425	2	2	6	5	4	4
30	0.1	−0.6	2	6	6	5	4	4
31	0.6	0.1	3	5	5	4	6	5
32	−0.5	−0.8	1	2	4	4	3	3
33	−0.2	−0.9	2	3	5	3	6	6
34	0.65	0.575	5	4	5	4	2	3
35	0.3	0.05	2	2	2	4	6	5
36	−0.6	−0.15	2	5	3	3	6	4
37	−0.8	−0.95	1	3	3	3	6	5
38	−0.25	−0.65	6	5	6	4	3	2
39	−0.25	0.25	2	4	4	2	6	5
40	−0.3	0.15	1	5	2	5	6	5
41	0.65	0.25	1	3	1	1	7	6
42	−0.55	N/A	1	N/A	2	N/A	6	N/A
43	0.7	0.15	2	2	5	4	5	5
44	−0.35	−1.1	1	6	5	5	6	5
45	0.35	0.875	1	3	6	3	2	2
46	0.55	−0.65	2	1	1	3	7	6
47	0.05	0.125	1	4	5	2	3	3
48	0.05	−0.2	2	3	2	4	5	5
49	0.4	0.95	2	2	5	3	4	4
50	0.35	−0.25	5	1	1	5	7	4
51	0.2	0.95	1	1	1	2	7	6

IAP, intrinsic attention to pain. N/A, not applicable.

Table S2. Peak MNI coordinates for regions that were significantly activated and deactivated during painful stimulation preceding reports of attention to pain

Region	*Z*-max	Peak voxel, MNI coordinates		
		x	*y*	*z*
Activation: attention to pain				
Insular cortex				
R aINS	7.85	36	14	−6
L aINS	7.19	−30	18	4
L aINS	7.06	−38	14	−6
R mINS	7.30	36	2	4
R pINS/S2	6.77	42	−18	12
Cingulate cortex				
MCC	7.02	6	22	32
PCC (anterior)	6.48	−4	−20	26
Temporoparietal junction				
R TPJ	6.58	54	−44	38
Frontal lobe				
L dlPFC	6.51	−32	42	16
R dlPFC	7.71	42	40	20
L middle frontal gyrus	5.81	−44	20	32
R frontal pole	7.04	26	46	18
R precentral gyrus	6.69	36	6	34
Parietal lobe				
L superior parietal lobule	6.75	−30	−58	40
R precuneus	4.90	14	−68	34
L precuneus	4.41	−8	−72	36
R postcentral gyrus (S1)	6.65	42	−22	44
Temporal lobe				
R lateral temporal cortex	5.31	56	−36	−14
L lateral temporal cortex	4.45	−54	−36	−12
Occipital lobe				
R lingual gyrus	8.41	10	−88	−4
Brainstem				
Midbrain	6.80	18	−26	−8
Cerebellum				
L crus I	7.43	−40	−60	−34
Deactivation: attention to pain				
Frontal lobe				
mPFC	5.08	−6	60	−8
L superior frontal gyrus	4.48	−22	16	30
Cingulate cortex				
PCC/precuneus	5.74	−8	−58	10
Parietal lobe				
L postcentral gyrus	5.97	−18	−30	54
L postcentral gyrus	3.89	−42	−18	36
R precuneus	4.00	12	−58	60
R postcentral gyrus	5.10	14	−28	60
Occipital lobe				
L lateral occipital cortex	5.53	−46	−78	24
Temporal lobe				
L fusiform gyrus	5.58	−26	−40	−18
R fusiform gyrus	5.72	22	−38	−20
Subcortical regions				
R hippocampus	3.62	26	−14	−20

Coordinates are in mm. Family-wise error corrected at $Z > 2.3$, cluster-based threshold of $P < 0.05$. The image was thresholded sequentially at $Z > 3$, $Z > 4$, $Z > 5$, $Z > 6$, and $Z > 7$ to obtain peak coordinates for clusters in focal regions. See Fig. S1 for visualization of full cluster extensions into additional regions. aINS, anterior insula; dlPFC, dorsolateral prefrontal cortex; L, left; MCC, midcingulate cortex; mINS, middle insula; pINS, posterior insula; R, right; S1, primary somatosensory cortex; S2, secondary somatosensory cortex; TPJ, temporoparietal junction.

Table S3. Peak MNI coordinates for regions that were significantly activated during painful stimulation preceding reports of attention to something other than pain

Region	*Z*-max	Peak voxel, MNI coordinates		
		x	*y*	*z*
Insular cortex				
R pINS/S2	6.77	44	−20	12
L aINS/operculum	6.11	−48	14	−10
R aINS	6.64	36	12	−6
R mINS/operculum	6.48	48	−4	2
Cingulate cortex				
MCC	6.16	−4	14	44
Frontal lobe				
R precentral gyrus	6.77	−36	−8	48
L frontal pole	6.20	−34	56	6
L dlPFC	5.93	26	48	18
L precentral gyrus	6.44	46	4	32
Parietal lobe				
R superior parietal lobule	5.70	34	−62	38
L superior parietal lobule	6.91	−28	−62	46
R postcentral gyrus (S1)	6.57	42	−22	44
Temporal lobe				
L middle temporal gyrus	5.12	−46	−50	0
L parahippocampal gyrus	5.07	−22	−32	−8
Occipital lobe				
L lingual gyrus	9.20	−10	−88	−8
Subcortical/brainstem regions				
Midbrain	6.85	18	−30	−8
Putamen	6.54	14	14	−6
Cerebellum				
L crus 1	6.99	−38	−62	−32

Family-wise error corrected at $Z > 2.3$, cluster-based threshold of $P < 0.05$. The image was thresholded sequentially at $Z > 3$, $Z > 4$, $Z > 5$, $Z > 6$, and $Z > 7$ to obtain peak coordinates for clusters in focal regions. See Fig. S1 for visualization of full cluster extensions into additional regions. No regions exhibited significant deactivation for this contrast.

Table S4. Peak MNI coordinates for regions that exhibited greater activation during painful stimulation periods preceding reports of attention to pain compared with periods preceding reports of attention to something other than pain

Region	*Z*-max	Peak voxel, MNI coordinates		
		x	*y*	*z*
Insular cortex				
R dorsal aINS	4.03	42	18	0
L dorsal aINS	3.87	−32	20	4
L mINS	3.31	−34	0	6
L vaINS	3.51	−38	−10	−12
R mINS/operculum	4.11	40	4	12
Frontal lobe				
R dlPFC	4.87	44	54	4
L opercular cortex	4.18	−54	2	6
R inferior frontal gyrus	4.16	60	12	2
Temporoparietal junction				
R TPJ/S2	3.95	54	−42	46
Parietal lobe				
R superior parietal lobule	3.44	40	−42	60

Family-wise error corrected at $Z > 2.3$, cluster-based threshold of $P < 0.05$. The image was thresholded sequentially at $Z > 2.3$, $Z > 3$, and $Z > 3.7$ to obtain peak coordinates for clusters in focal regions. See Fig. 3*A* for visualization of full cluster extensions into additional regions.

Table S5. Peak MNI coordinates for regions that exhibited greater activation during painful stimulation periods preceding reports of something other than pain compared with periods preceding reports of attention to pain

Region	*Z*-max	Peak voxel, MNI coordinates		
		x	*y*	*z*
Frontal lobe				
mPFC	5.07	−2	58	−6
R superior frontal gyrus	4.08	22	30	36
R paracingulate gyrus	4.85	−18	16	36
L paracingulate gyrus	3.84	−14	42	16
Parietal lobe				
L postcentral gyrus	4.69	−48	−14	30
Cingulate cortex				
PCC/precuneus	5.17	6	−56	2
L PCC/precuneus	4.85	12	−58	10
Subgenual ACC	4.90	0	16	−6
L retrosplenial cortex	4.88	−10	−52	0
Temporooccipital junction				
R TOJ	4.73	44	−64	16
L TOJ	5.13	−46	−76	24
R temporal/occipital fusiform cortex	4.07	38	−62	−10
Temporal lobe				
L lateral temporal cortex	4.01	−62	−12	−18
L fusiform gyrus/parahippocampal cortex	4.33	−28	−42	−12
R fusiform gyurs	4.11	30	−42	−16
Occipital lobe				
L intracalcarine cortex/lingual gyrus	4.47	−12	−82	2
Subcortical regions				
R hippocampus	3.34	30	−20	−16

Family-wise error corrected at $Z > 2.3$, cluster-based threshold of $P < 0.05$. The image was thresholded sequentially at $Z > 2.7$, $Z > 3.3$, $Z > 4$, and $Z > 4.7$ to obtain peak coordinates for clusters in focal regions. See Fig. 3*B* for visualization of full cluster extensions into additional regions. ACC, anterior cingulate cortex; TOJ, temporooccipital junction.

Table S6. Peak MNI coordinates for regions that exhibited greater FC with the PAG area during painful stimulation periods preceding reports of something other than pain compared with periods preceding reports of attention to pain

Region	*Z*-max	Peak voxel, MNI coordinates		
		x	*y*	*z*
Frontal lobe				
mPFC	3.66	−4	52	6
Middle frontal gyrus	3.49	−40	0	52
Retrosplenial cortex	3.23	−6	−50	2
Temporal lobe				
L parahippocampal gyrus	4.08	−14	−36	−8
Subcortical regions				
L hippocampus	3.34	−26	−26	−14

Identified with psychophysiological interaction analysis. Family-wise error corrected at $Z > 2.3$, cluster-based threshold of $P < 0.05$. The image was thresholded sequentially at $Z > 2.3$ and $Z > 3$ to obtain peak coordinates for clusters in focal regions. FC, functional connectivity.

Table S7. Individual accuracy and mean reaction time and SD for 51 subjects for the cognitive interference task for pain and no-pain conditions

	Accuracy, %		RT, ms (correct trials)			
Subject	Pain	No pain	Mean (pain)	SD (pain)	Mean (no pain)	SD (no pain)
1	89.583	90.625	1,061.3	235.17	1,134.2	265.27
2	92.708	94.792	1,327.5	269.94	1,355.6	323.69
3	96.875	95.833	1,196	222.16	1,278.1	270.5
4	98.958	98.958	980.69	181.73	1,045	212.68
5	97.917	95.833	1,306.7	209.24	1,348.2	259.48
6	80.208	83.333	1,539.4	334.29	1,134.1	288.5
7	96.875	96.875	1,222.8	285.19	1,268.4	309.78
8	57.292	47.917	1,718.4	446.36	1,694.3	435.64
9	97.917	92.708	1,412.8	307.08	1,397.8	300.77
10	82.292	79.167	1,339.9	375.71	1,323.9	391.15
11	97.917	95.833	1,222.6	271.44	1,355.1	362.4
12	95.833	92.708	1,490.9	381.76	1,464.7	322.33
13	97.917	96.875	998.95	230.08	1,078.3	314.04
14	96.875	95.833	940.38	180.8	888.54	187.91
15	88.542	93.75	1,006	182.44	1,107.8	276.14
16	76.042	73.958	1,640	403.77	1,674.5	365.05
17	94.792	95.833	1,179	255.85	1,173.5	302.63
18	97.917	97.917	1,066.2	177.44	1,055.6	204.76
19	96.875	86.458	1,245.7	273.11	1,274.7	270.36
20	98.958	97.917	1,347	259.72	1,275.4	246.7
21	97.917	97.917	1,307.8	241.57	1,398.3	267.48
22	97.917	96.875	991.99	185.07	1,061.8	201.29
23	96.875	98.958	1,125.4	244.1	1,196.6	274.55
24	92.708	95.833	911.57	229.89	957	230.38
25	97.917	97.917	1,014.9	134.95	1,059.2	165.02
26	97.917	96.875	1,044	215.41	1,000.4	233.55
27	92.708	94.792	1,330.5	257.2	1,301.6	272.32
28	N/A	N/A	N/A	N/A	N/A	N/A
29	90.625	92.708	1,387.2	386.8	1,372.5	334.98
30	96.875	95.833	1,103.7	157.79	1,102.7	164.64
31	97.917	94.792	999.4	158.88	1,035.8	188.53
32	96.875	96.875	835.93	139.41	892.46	209.75
33	95.833	93.75	1,066.2	297.6	1,224.7	425.45
34	93.75	94.792	1,144.5	203.51	1,185.7	248.72
35	85.417	85.417	805.27	149.49	848.18	169.27
36	89.583	81.25	1,389.5	300.55	1,539.7	367.86
37	92.708	94.792	858.94	195.23	973.13	231.55
38	100	98.958	928.89	159.85	959.75	169.92
39	94.792	94.792	1,288.5	288.27	1,340.1	267.08
40	93.75	95.833	1,260.2	310.33	1,209.3	264.91
41	95.833	97.917	1,006.8	226.42	1,051.2	236.48
42	94.792	98.958	950.29	181.8	977.53	202.81
43	90.625	82.292	1,276.7	346.29	1,466.8	417.14
44	100	97.917	1,072.4	248.6	1,134	255.49
45	98.958	97.917	929.34	172.1	991.18	215.21
46	96.875	93.75	874.7	139.65	887.47	161.08
47	91.667	88.542	1,163.7	254.3	1,180.2	270.36
48	97.917	96.875	1,184.1	202.98	1,236.5	235.41
49	98.958	100	1,173.4	223.31	1,236.9	244.01
50	96.875	95.833	1,156	191.68	1,157.1	220.93
51	100	98.958	1,285.1	219.42	1,322.8	212.4

Ninety-six total trials each per subject.

Table S8. Effect of the sliding window duration used to calculate FCV on the correlation between IAP (session 1) and mPFC–PAG FCV during the resting state scan in 51 subjects

Sliding window duration, s	Group mean ± SD mPFC–PAG FCV	Correlation with IAP (*r*)	Correlation with IAP (*P* value)
30	1.39 ± 0.173	−0.281	0.045
40	1.17 ± 0.176	−0.318	0.023
50	1.00 ± 0.178	−0.323	0.021
60	0.87 ± 0.176	−0.310	0.027

Shorter windows are associated with greater FCV, as expected, but the correlation between FCV and IAP remains consistent regardless of window duration. FCV, functional connectivity variability.